High-frequency Si/SiGe phototransistor model: Operation on multiple polarization points

A.M. DIOP[1], A. BENNOUR[2], S MAZER[3], M. EL BEKKALI[4]

[1]IASSE Laboratory , University Sidi Mohamed Ben Abdellah Fès, Maroc

M. FATTAH[2]

[2]IMAGE Laboratory, Moulay Ismail1University Meknes, Morocco

J-L. POLLEUX[3]

[3]University Paris-Est, ESYCOM (EA 2552), ESIEE, UPEM, Le Cnam, Noisy-le-Grand, France.

C. ALGANI[4]

[4]Le Cnam, ESYCOM (EA2552), Paris, France

Abstract. This article presents the results of our research on the modeling of an HPT SiGe heterojunction phototransistor. Usually this HPTs type work for a single point of polarization in this work, we were interested in modeling the same HPT on different points of polarization. We will model the HPT to operate at both 2V and 3V, so that we can use the HPT at multiple bias points and reduce costs and allow the reuse of the HPT SiG heterojunction phototransistor on further studies. For a defined point of polarization we will optimize the operation of the HPT so that it flies with the dynamic measurements and we will not base on this HPT by modifying certain values and components so that the HTP works on the other points of polarization.

Keywords: HPT heterojunction phototransistor, RoF Radio-over-fiber

1   Introduction

Today 4G has already shown its limits in terms of connection speed, latency which is the time it takes for data from source to destination. It rises by 50 ms [1]. The number of connected objects has been on the rise for several years. Satatista estimates the number of connected objects at 75.44 billion in 2025 [2]. This increase creates the need for greater bandwidth, very high throughputs and much lower latency. 5G makes it possible to respond well to this need. In view of the constitution of the 5G networks: several mobile radio cells and the fiber optic infrastructure currently in place, it is essential to set up a network that can combine the two, this will be the advent of 6G. Currently Radio-over-fiber (RoF) seems to be suitable.

5G will initially operate on a frequency band of 3.4 GHz to 3.8 GHz but frequencies of 700 MHz will be used to deport the 5G signal in rural areas (large range) or frequencies of 26 GHz for urban areas [3].
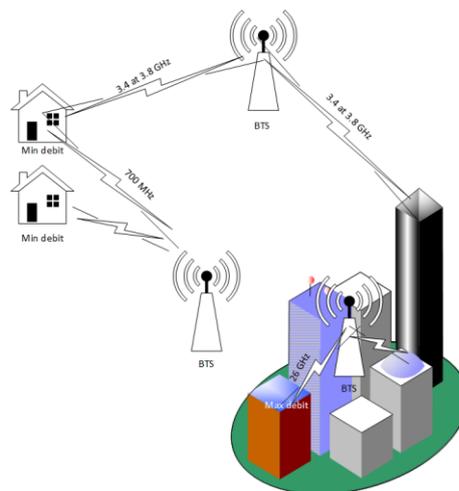

Fig. 1. Frequency required on 5G deployment

In urban areas to guard against losses in free space and maintain very high speed, optical fiber will be at the heart of 5G infrastructure. fiber will connect radio stations, base station antennas to microcells.

Fig. 2. shows the evolution of the 5G signal in the RoF architecture. The data is converted to a baseband signal, then converted to RF which will be applied to the input of the RoF (Radio over Fiber) block. The optical wave coming out of the fiber is converted back into an RF signal which will be propagated on the radio interface using an antenna [4]
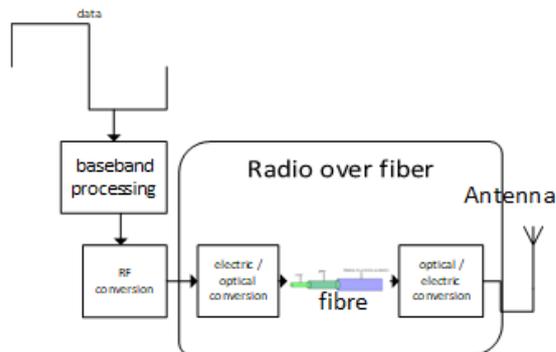

Fig. 2. 5G uplink data transmission

The optical to electrical signal conversion block is mainly composed of phototransistor.

HPT phototransistors absorb light exiting the optical fiber through the base, which they convert into electrons. The electrons thus obtained will be injected into the collector and the resulting holes in the base which will generate a photo-current in the base. The latter will be amplified by the transistor effect.

We have several types of phototransistors in the market: Germanium, Indium Gallium Arsenide, Lead (II) Silicon Sulfide. Among the existing phototransistors, the one which is characterized by a very low manufacturing cost and a good quality / price ratio remains the one based on silicon Si / SiGe phototransistor. It is for these reasons that we adopted this technology for our modeling work.

In order to be able to test and validate the measurements taken in the ESYCOM laboratory , we are going to model an Si / SiGe HPT which allows the measurements to be reproduced. Work has already been carried out in the IASSE lab (formerly called LTTI) in collaboration with ESYCOM to validate the use of HPT Si / SiGe $V_{CE} = 2\ V$ and $V_{BE} = 0.81\ V$ [5]. The work presented in this paper aims to extend the use of this same HPT to other points of polarization: VCE=3 V and V_BE=0.69 V.

2   Description of the HPT model and 2V optimization

The HPT used will be the TELEFUNKEN GMBH SIGE2-RF Bipolar Technology HPT 10SQxEBC [6]. Figure 3 shows a profile cup of the HPT.
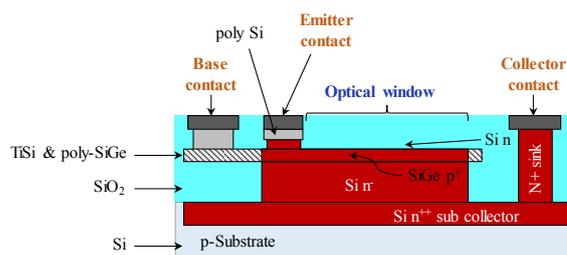

Fig. 3. HPT 10SQxEBC Profile Cut

The HPT model made is based on the Model of Ebers & Moll 3.

The HPT 10SQxEBC is composed of an optical window of 10x10μm2 the shape of the window is given by the letters SQ here we have a square optical window on an extended basic structure which does not imply extra work for the realization of the realization of the realization of the Optical window. EBC letters will give the type of the optical window: extended collector base transmitter.

The study of the HPT 10SQxEBC model can be carried out modularly which allows a separate component study of HPT. Each group of component is studied independently of others which gives a certain advantage and greatly facilitates the study. Dynamic parameters can be observed independently of static and dynamic parameters.

Previous studies have been done on the HPT 10SQxEBC by the laboratory in collaboration with ESYCOM to validate the work of the HPT to $V_{CE} = 2\ V$. The phototransistor based on the model of Ebers & Moll 3 used allows

to model the HPT 2V. Each new polarization point requires an adaptation of the values of the different parameters of the HPT. We will define a model that will operate on several polarization points.

For a given polarization point taking into account the propagation of the waves, we will consider the HPT 10SQxEBC as a quadrupole Fig. 4.

Fig. 4. Representation of incident waves and reflected at access of a quadrupole

The parameter matrix will result from the relationships between the waves.

The equation of parameters will write in the form:

$$\begin{pmatrix} b_1 \\ b_2 \end{pmatrix} = \begin{bmatrix} S_{11} & S_{12} \\ S_{21} & S_{22} \end{bmatrix} \begin{pmatrix} a_1 \\ a_2 \end{pmatrix} \tag{1}$$

The study that will be carried out later will focus mainly around the coefficient of direct transmission commonly called gain.

$$S_{21} = \left. \frac{b_2}{a_1} \right|_{a_2=0} \tag{2}$$
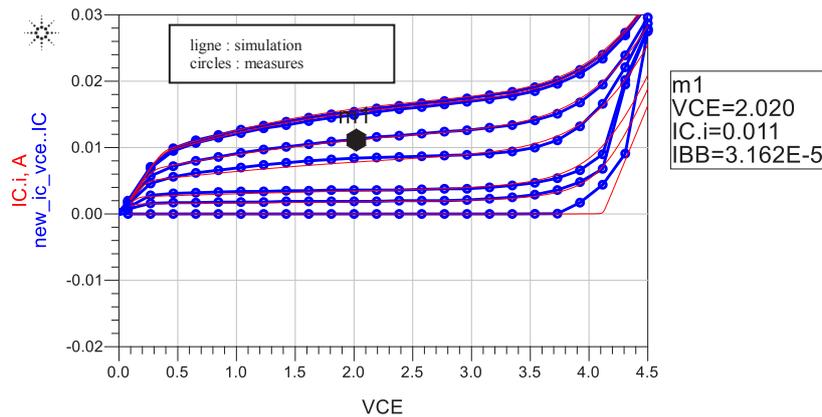
Fig. 5. Polarization point scheme $V_{BE} = 0.81\ V$ and $V_{CE} = 2\ V$

Fig. 5 is composed of two curves we have the measurements not provided the ESYCOM laboratory in a circle we have superimposed the results of the modeling of the HPT in order to show the good agreement between the measurements and the simulations we have obtained after the different Optimizations of the modeling of the static part of the HPT. The contiguity of the simulations on the measurements allows us to deduce that the HPT is well modeled in the static mode. Figure 5 makes it possible to determine the polarization points of the HPT. For a polarization point in $V_{CE} = 2V$ We will depend on the measures available choose the value of $V_{BE} = 0.81V$ affected a modeling of the gain S_{21}

Fig. 6 below shows the optimization of the modeling of parameter S_{21} which will represent the gain of the HPT at the polarization point $V_{BE} = 0.81V$ and $V_{CE} = 2V$ in functions of the measurements of the gain of the HPT.
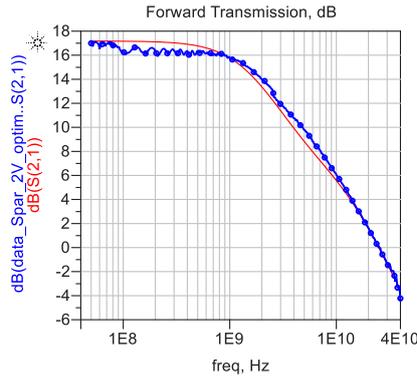
Fig. 6. Optimization of S parameters for a HPT 10SQxEBC $V_{BE} = 0.81\,V$ and $V_{CE} = 2\,V$

According to Fig. 6 representing the parameter S_{21}, We find that there is a very good correspondence between the measurement and modeling results which allows us to deduce that the HPT is well modeled in dynamic mode.

The work that is carried out later will be to tuner the parameters of the HPT in order to obtain the validity domain at the polarization point $V_{BE} = 0.81\,V$ and $V_{CE} = 2\,V$.
Fig 7 shows the 10SQxEBC electrical diagram it is composed of an extended and active zone which forms the HPT of a substrate. The extended and active zone are constructed of ways that the study of static, optical and dynamic parameters can be differentiated. In this paper we are going focus on the dynamic parameters that will be introduced by the different junction and junction and broadcast capabilities:
Basic collector junction capacity:

$$C_{jC} = \frac{C_{jC0}}{(1 - F_c)^{(m_C+1)}} * \left[1 - F_c * (1 + m_C) + m_C \frac{V_{B'C'}}{V_d} \right] \tag{3}$$

Basic transmitter junction capacity

$$C_{jE} = \frac{C_{jE0}}{(1 - F_c)^{(m_E+1)}} * \left[1 - F_c * (1 + m_E) + m_E \frac{V_{B'E'}}{V_d} \right] \tag{4}$$

Impact of depletion of the junction base-collector

$$C_{dC} = \frac{\tau_R * I_S}{n_R * V_T * N_{qb}} * \left[e^{\frac{V_{B'C'}}{n_R * V_T}} \right] \tag{5}$$

Ability to deplete the base transmitter junction

$$C_{dE} = \frac{\tau_F * I_S}{n_F * V_T * N_{qb}} * \left[e^{\frac{V_{B'E'}}{n_F * V_T}} \right] \tag{6}$$

Capacities guarded the same expressions in the extended field "e" that in the active field "A".
with: V_T thermal voltage, C_{jX0} capacity for a $V_{B'X'} = 0$ V, $V_{B'X'}$ the internal potential of the junction, m_X is an adjustment factor, V_d is the diffusion potential, Fc point where the linearization of the function begins, nF and nR the coefficients of forward and reverse ideality, ideal transit time reverse τR et τ_F ideal transit time forward, N_{qb} factor of the load in the base and IS saturation current.
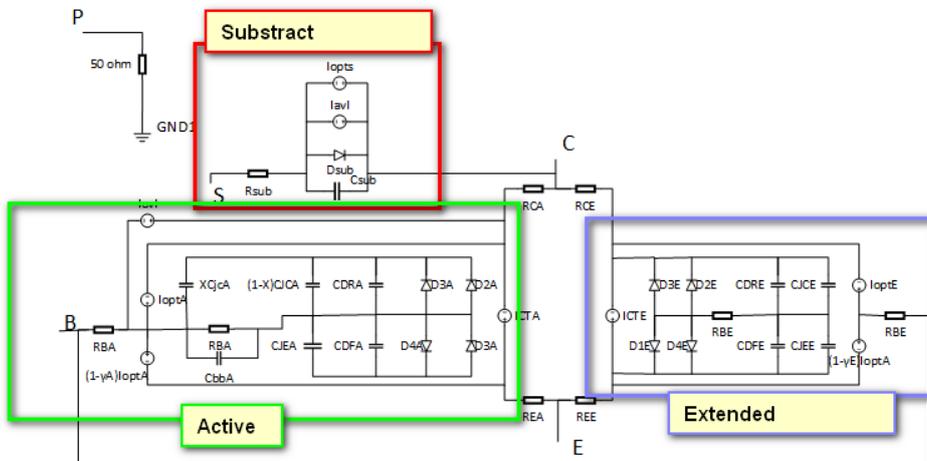
Fig. 7. Electrical representation of PTH 10SQxEBC

3   Modelization HPT at 2V and 3V

We will represent the measure obtained for the polarization point of $V_{CE} = 3\,V$ and $V_{BE} = 0.69V$ on the curve that allows us to model the $V_{CE} = 2\,V$ and $V_{BE} = 0.81\,V$ one fig. 8.
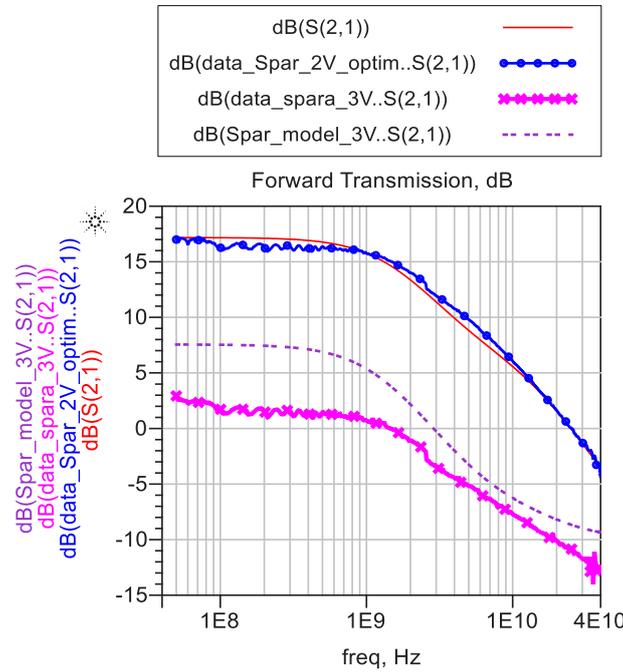

Fig. 8. Modeling representation to 2V and 3V

Fig. 8 shows the gain S_{21} of the HPT on the polarization points 2V and 3V. Circle and Online Curves continues gives 2V HPT modeling. These two curves are obtained by focusing that on the 2V. Cross curve (measurements) and dash (simulation fixed) represents the gain S_{21} et 3 V Keeping the same capabilities values as for 2 V modeling. We observe a gap between measurements and simulation. We will solve this problem by optimizing the values of the components of our model so that it is operational at other polarization points.

We will start by manually tuning the dynamic parameters of the capabilities defined in equations 3 to 6 to 2V in order to frame the different parameters of the HPT 10SQxEBC.

Table 1 represents the values obtained after tuning of the various components by accepting a certain degree of freedom for the point of polarization 2V.

TABLE 1. Minimum and maximum value possible of dynamic parameters for $V_{BE} = 0.81\,V$ *and* $V_{CE} = 2\,V$

Symbole	min	max
V_F (V)	0.6485	0.9825
	0.6485	
M	0.294	0.803104
	0.294	
C_{jC0}	2.11e-018	2.44003e-14
X	0. 35	1.00235
V_F (V)	0.373607	0.822
M	0.69792	0.773
C_{jE0}	0.981831e-16	1.51145e-13

The objective is to supervise the different terms of the capacities that will allow us to always validate the functioning of HPT 10SQxEBC at $V_{CE} = 2\,V$ and $V_{BE} = 0.81\,V$.

After framing the values of the parameters of the junction and diffusion capabilities. We will change the polarization point to VBE=0.69 V and VCE=3 V, Then optimize the junction and diffusion capacities while remaining in the validity range defined in Table 1. Finally we get Figure 9 that validates the operation of the phototransistor to $V_{CE} = 2\,V$, $V_{BE} = 0.81\,V$ and VBE=0.69 V, VCE=3 V.

Fig. 9b shows the optimization of dynamic gain S_{21} of the HPT on $V_{CE} = 2\,V$, $V_{BE} = 0.81\,V$ and Figure 9a shows the optimization of dynamic gain S_{21} of the HPT VBE=0.69 V, VCE=3 V Depending on the measurements made by the ESYCOM laboratory, for the same parameters of the junction and diffusion capacity.
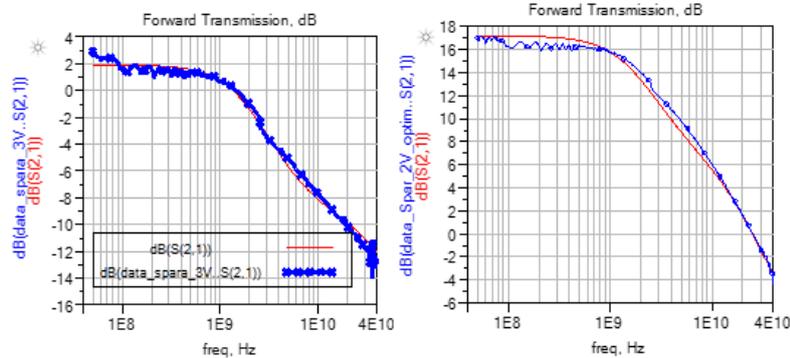

Fig. 9a : Optimisation des paramètres S pour un HPT 10SQxEBC $V_{BE} = 0.69\,V$ et $V_{CE} = 3\,V$

Fig. 9b : Optimisation des paramètres S pour un HPT 10SQxEBC $V_{BE} = 0.81\,V$ et $V_{CE} = 2\,V$

We see a fairly good concordance at once at 2V and 3V between measurements and simulations. We can conclude that the model is operational not just 2 V, but also to 3V. As a prospect, we will expand the functioning of our model at other polarization points namely 4V and 5V, to offer a wider range of the HPT 10SQxEBC.

Conclusion

The research carried out on the HPT 10SQxEBC particularly on the dynamic aspect has led to good results on the possibilities of using the same HPT for several different polarization points. Similar work will continue to determine the limits of HPT 10SQxEBC in its operation in the dynamic and optical field We will also try to generalize the HPT model on other points of polarization.

Références

1. F. Lecoche, Transmission Quality Measurement of Two Types of 60 GHz Millimeter-Wave Generation and Distribution Systems, Journal of Lightwave Technology, vol.27, issue.23, pp.5469-5474, 2009.
2. Internet of Things (IoT) connected devices installed base worldwide from 2015 to 2025, Published by Statista Research Department, Nov 27, 2016.
3. Mamadou D. Balde , Joni Vehmas, Sinh L. H. Nguyen, Katsuyuki Haneda, Heykel Houas, Bernard Uguen "A 32 GHz Urban Micro Cell Measurement Campaign for 5G Candidate Spectrum Region", Published in : IEEE 2017 11th European Conference on Antennas and Propagation (EUCAP)
4. Kokou Firmin Fiaboe, 2Riyanka Bandyopadhyay, Pranaw Kumar "BER Analysis and Mitigation of Four-Wave Mixing effect in Radio over Fiber System" 2019 JETIR April 2019, Volume 6, Issue 4
5. Alae Bennour "Electric modeling Large signal from phototransistor sige in industrial technology for the design of integrated photonical circuit design low cost" Ph.D Thesis, Sidi Mohamed Ben Abdellah University - FES November 2017
6. Marc D. Rosales, Jean-Luc Polleux, Catherine Algani "Design And Implementation of Sige PTHS Using An 80GHz Sige Bipolar Process Technology "8th IEEE INTERNATIONAL CONFERENCE ON GROUP IV Photonic, pp. 243-245, London, seven 2011.